

## Supplementary information

### Significantly increased energy density and discharge efficiency at high temperature in polyetherimide nanocomposite by a small amount of Al<sub>2</sub>O<sub>3</sub> nanoparticles

Mingzhi Fan, Penghao Hu\*, Zhenkang Dan, Jianyong Jiang, Binzhou Sun, Yang Shen\*

Corresponding author

E-mail: [huph@ustb.edu.cn](mailto:huph@ustb.edu.cn); [shyang\\_mse@tsinghua.edu.cn](mailto:shyang_mse@tsinghua.edu.cn)

**Fig. S1**(a) presents the X-ray diffraction (XRD) patterns of the AO-nps, and all of the deflection peaks of the product are well indexed by the standard data of face-centered cubic  $\gamma$ -Al<sub>2</sub>O<sub>3</sub> (PDF#29-0063), indicating the high purity of the nanoparticles.

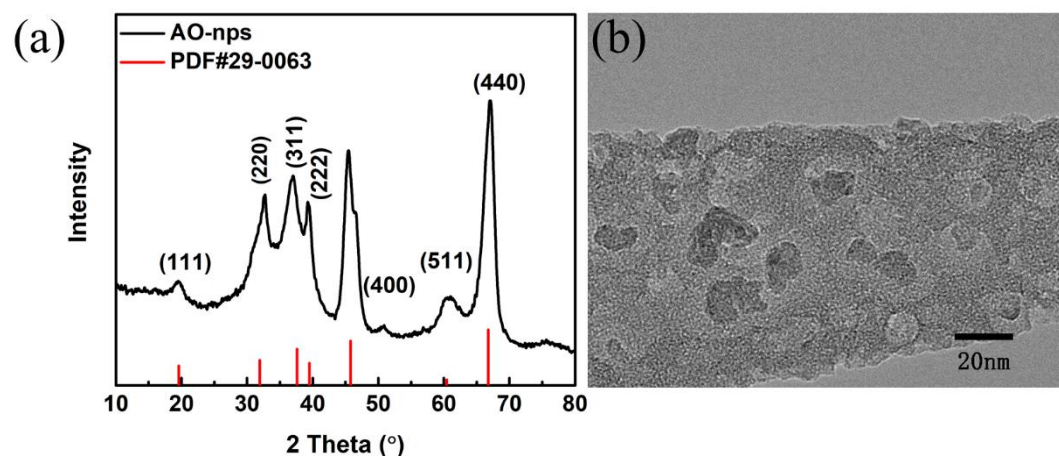


**Fig. S1.** (a) X-ray diffraction (XRD) patterns of the nanostructured Al<sub>2</sub>O<sub>3</sub> fillers. (b) TEM image of Al<sub>2</sub>O<sub>3</sub> particles.

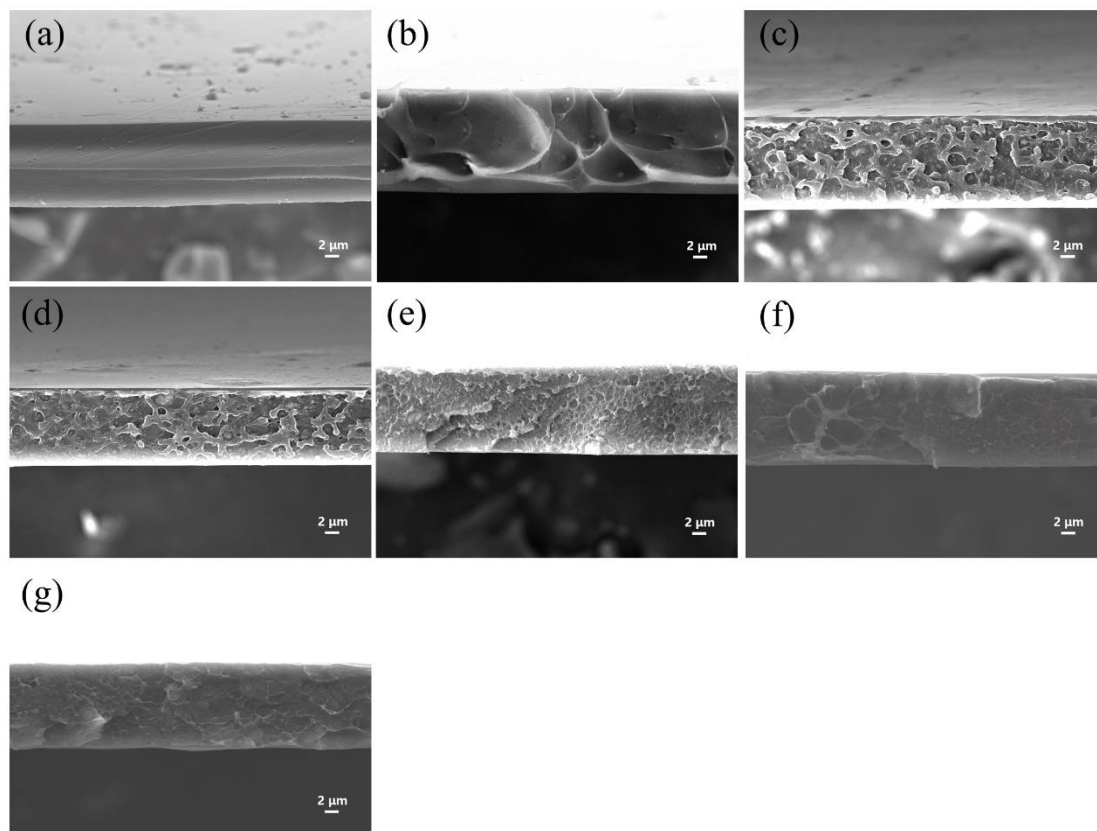


**Fig. S2.** Cross-sectional SEM images of (a) pure PEI film, (b) PEI nanocomposites with 0.5 vol% AO-nps, (c) PEI nanocomposites with 1 vol% AO-nps, (d) PEI nanocomposites with 2 vol% AO-nps, (e) PEI nanocomposites with 3 vol% AO-nps, (f) PEI nanocomposites with 5 vol% AO-nps, and (g) PEI nanocomposites with 7 vol% AO-nps.

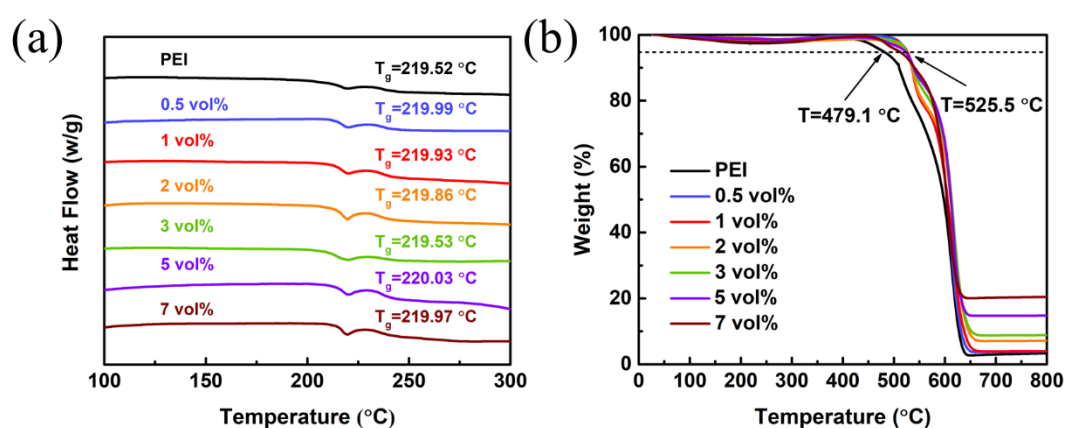


**Fig. S3.** (a) DSC and (b) TGA curves of pristine PEI and the PEI/AO-nps nanocomposite films.

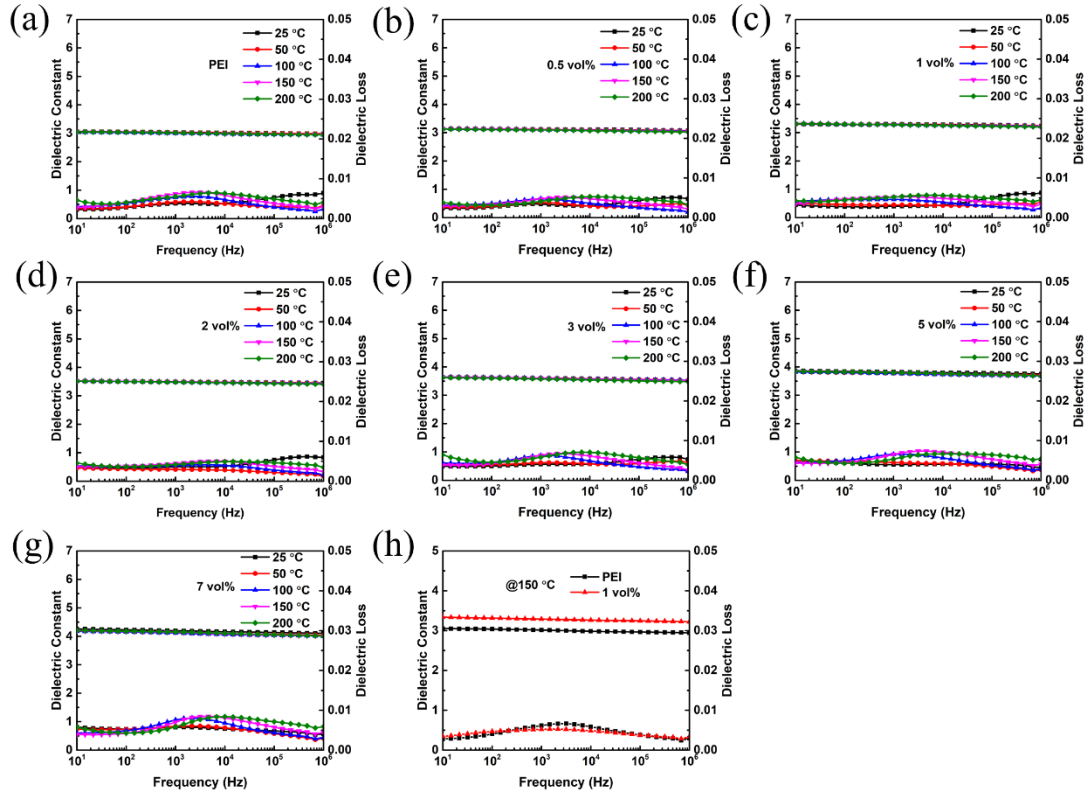


**Fig. S4.** Dielectric spectra of nanocomposites with varied frequency and temperature, (a) PEI, (b) 0.5vol%, (c) 1vol%, (d) 2 vol%, (e) 3 vol%, (f) 5 vol%, and (g) 7vol%. (h) Frequency-dependent dielectric properties of the PEI and PEI composite with 1vol% AO-nps at 150 °C.

**Table S1** Breakdown strength of PEI and nanocomposites with varied content measured at different temperature.

成分	25 °C		50 °C		100 °C		150 °C	
	$E_b$	$\beta$	$E_b$	$\beta$	$E_b$	$\beta$	$E_b$	$\beta$
	(MV/m)		(MV/m)		(MV/m)		(MV/m)	
PEI	558.1	16.9	558.1	14.5	500.3	13.0	421.8	6.5
0.5 vol%	567.7	15.7	562.6	17.3	516.0	13.8	445.3	8.0
1 vol%	581.7	19.4	575.9	18.5	548.2	16.6	503.9	11.1
2 vol%	571.3	20.1	566.1	20.1	527.2	19.3	456.8	7.4
3 vol%	544.9	16.5	543.4	16.7	511.1	13.2	430.8	6.4
5 vol%	428.7	13.0						
7 vol%	384.3	8.6						

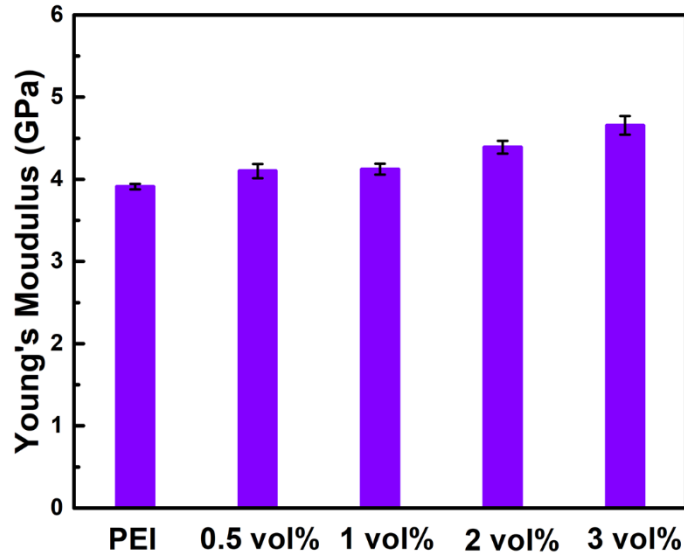


**Fig. S5.** Young's modulus of the nanocomposites with varied filler content measured at room temperature.

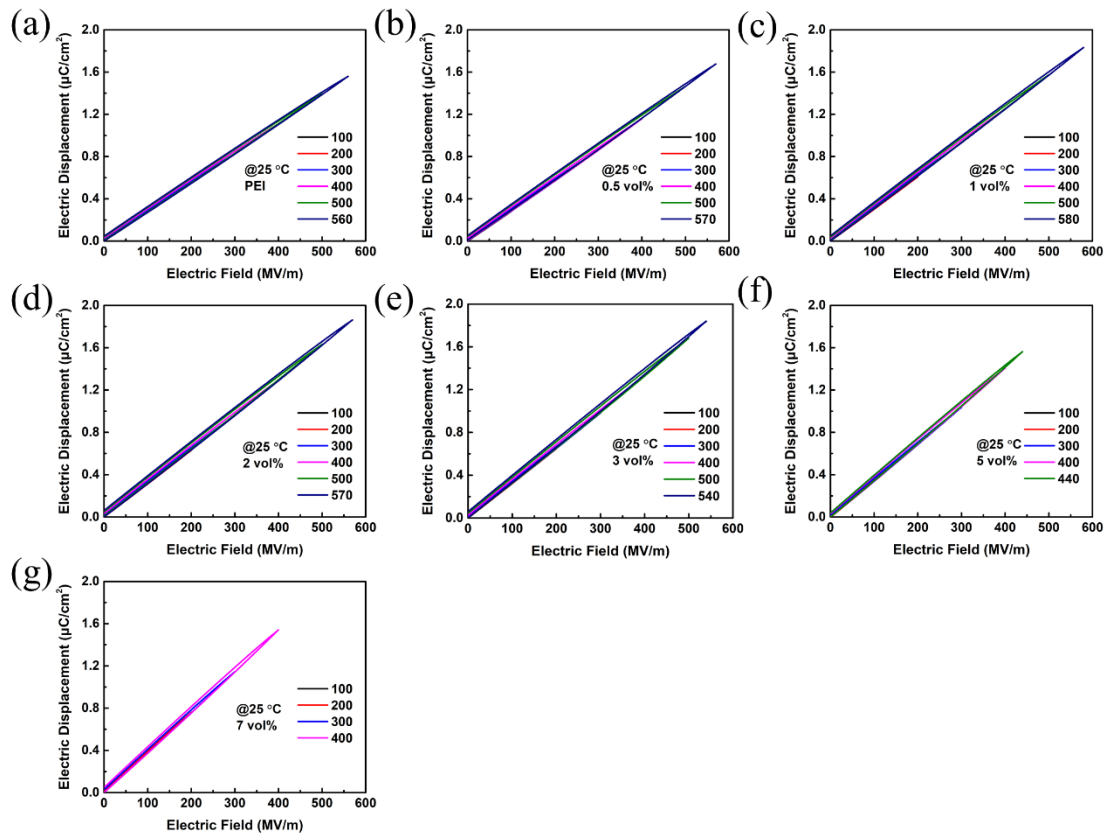


**Fig. S6.** Electric displacement-electric field (D-E) loops of nanocomposites with varied filler content measured at 25 °C, (a) PEI, (b) 0.5 vol%, (c) 1 vol%, (d) 2 vol%, (e) 3 vol%, (f) 5 vol%, and (g) 7 vol%.

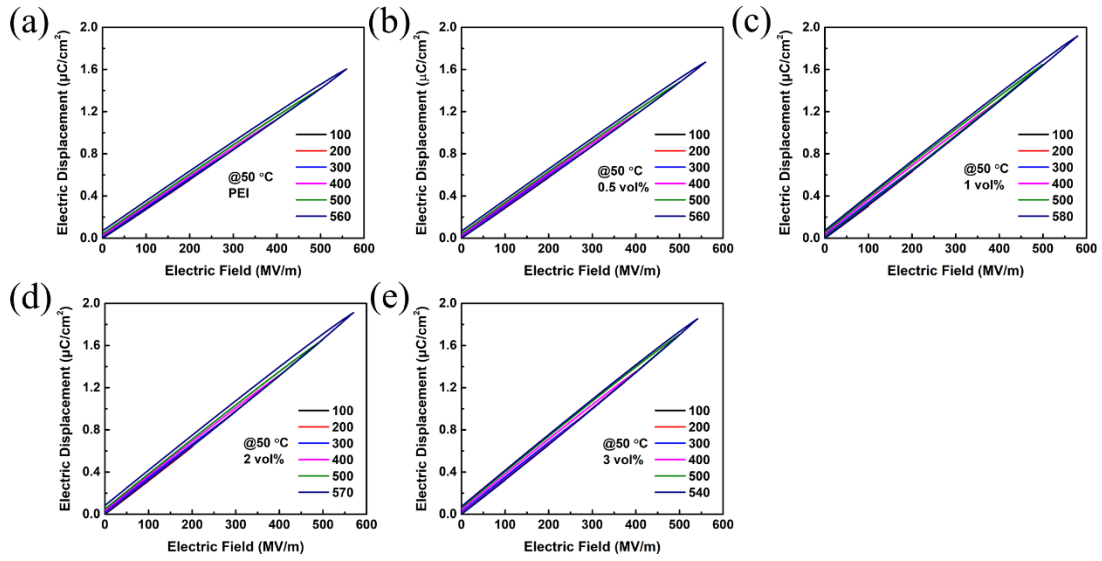


**Fig. S7.** Electric displacement-electric field (D-E) loops of nanocomposites with varied filler content measured at 50 °C, (a) PEI, (b) 0.5vol%, (c) 1vol%, (d) 2 vol%, and (e) 3 vol%.

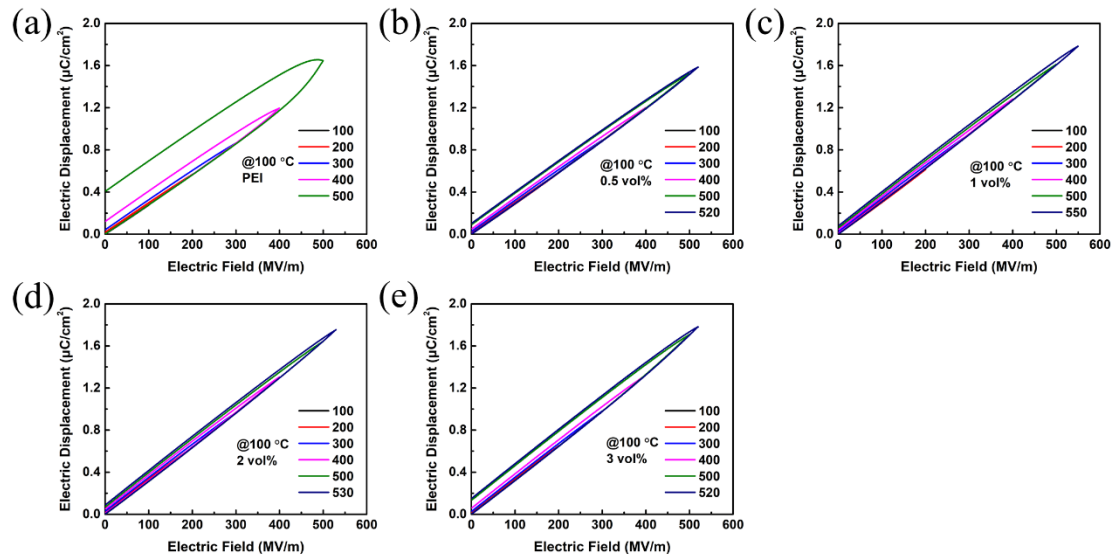


**Fig. S8.** Electric displacement-electric field (D-E) loops of nanocomposites with varied filler content measured at 100 °C, (a) PEI, (b) 0.5vol%, (c) 1vol%, (d) 2 vol%, and (e) 3 vol%.

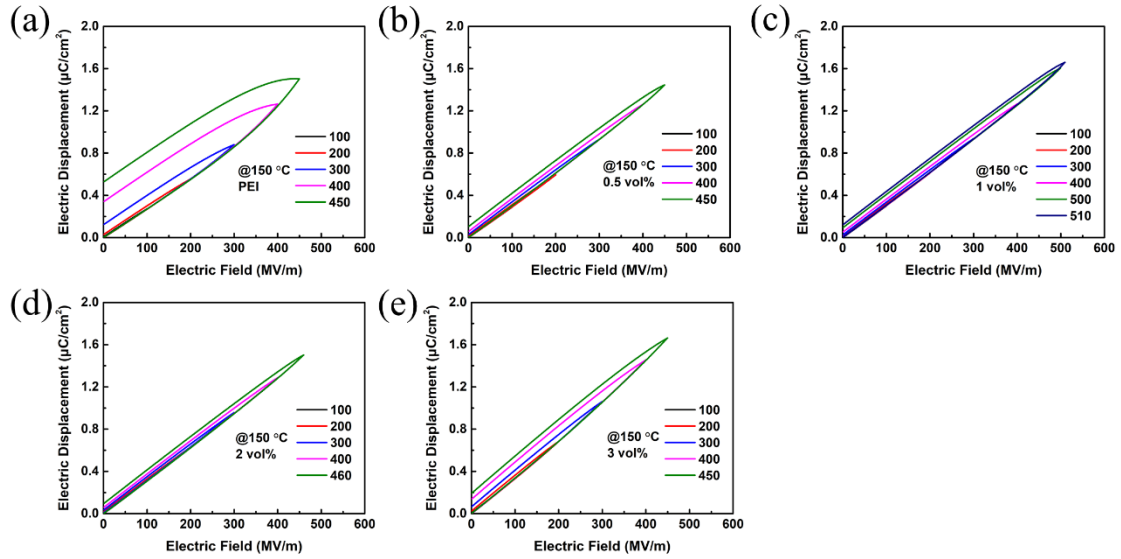


**Fig. S9.** Electric displacement-electric field (D-E) loops of nanocomposites with varied filler content measured at 150 °C, (a) PEI, (b) 0.5vol%, (c) 1vol%, (d) 2 vol%, and (e) 3 vol%.

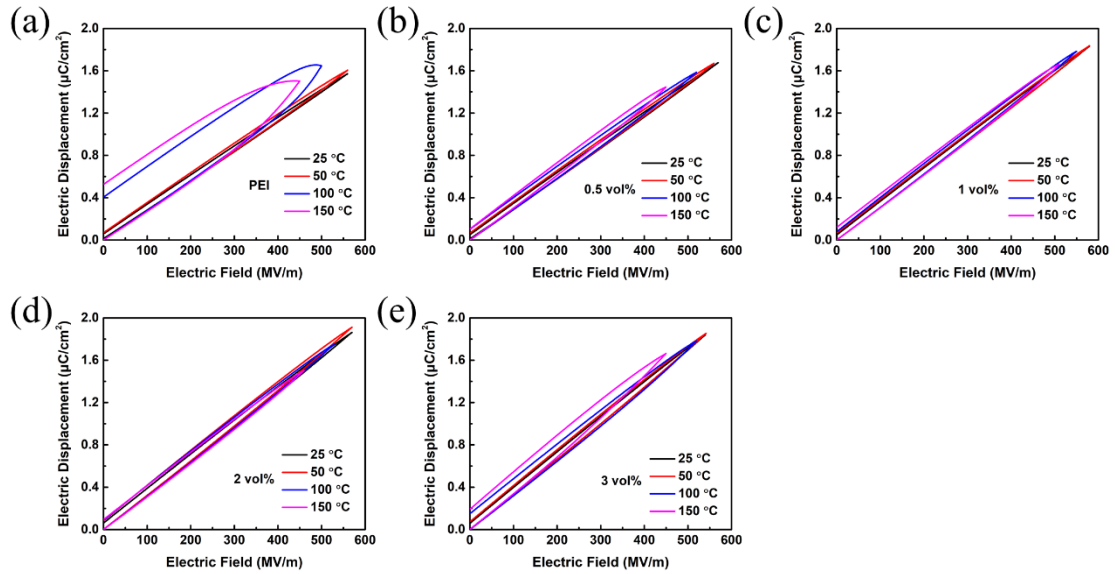


**Fig. S10.** Maximum electric displacement-electric field (D-E) loops of nanocomposites measured at different temperature, (a) PEI, (b) 0.5vol%, (c) 1vol%, (d) 2 vol%, and (e) 3 vol%.

**Fig. S11(a)** shows the TSDC spectroscopies of the nanocomposites, which are collected under a poling field ( $E_p$ ) of 15 MV/m for a poling time of 30 min at poling temperature ( $T_p$ ) of 150 °C. There is only a peak at 180-200 °C, which is supposed to

be ascribed to the depolarization of the injected charges from electrodes, i.e., Schottky or thermionic emission. As shown in **Fig. S11(b)** The  $E_p$ -dependent TSDC test was performed for PEI with 1 vol% AO-nps to verify the hypothesis about injection charges. In general, for Schottky emission, the current density ( $J$ ) scales as  $\ln J \propto E_p^{1/2}$ . At equilibrium state, the injected charges equal to the leakage charges ( $C$ ), which can be obtained from the TSDC spectrum as  $\ln C \propto E_p^{1/2}$ . **Fig. S11(c)** establishes the linear relationship between  $\ln C$  and  $E_p^{1/2}$ , which supports our prediction. The increase of maximum displacement and decrease of remnant displacement bring about considerable improvement in high-temperature electric energy storage.

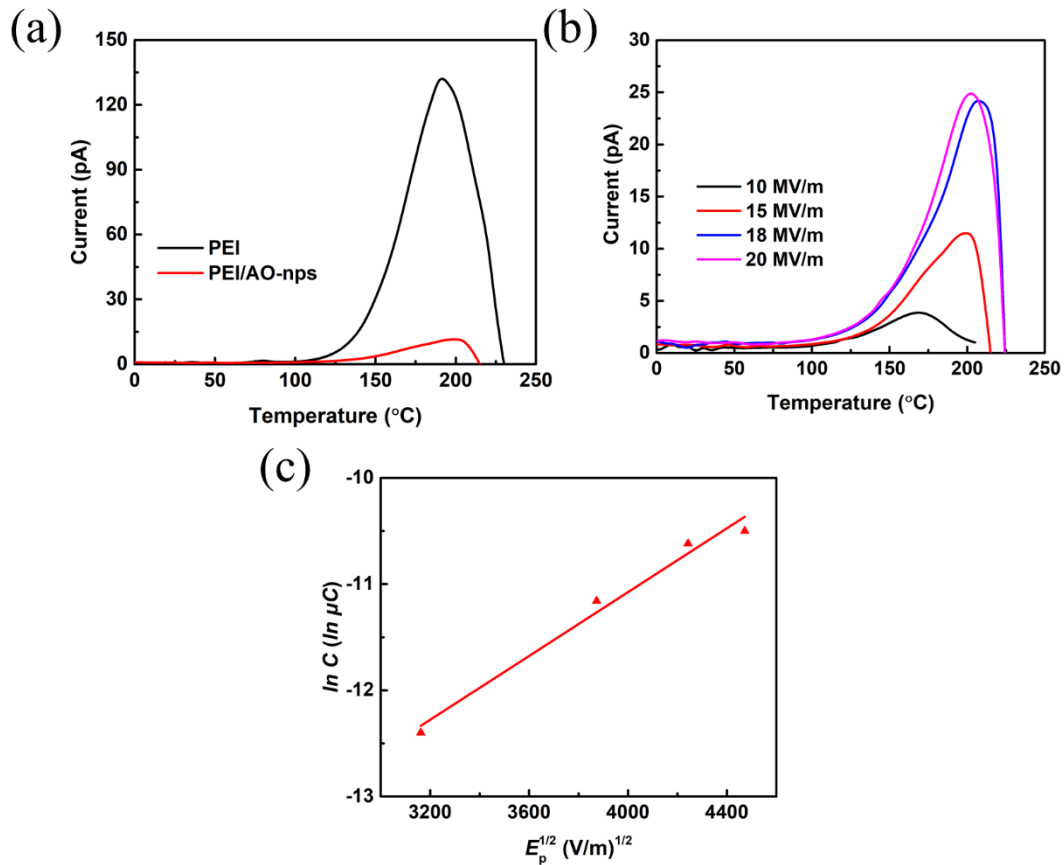


**Fig. S11.** (a) TSDC curves of PEI and PEI/AO-nps under poling electric field of 15 MV/m at 150 °C for 30 min. (b) TSDC spectra for PEI/AO-nps film under different poling electric field at 150 °C for 30 min. (c) The relationship between  $\ln C$  and  $E_p^{1/2}$ .

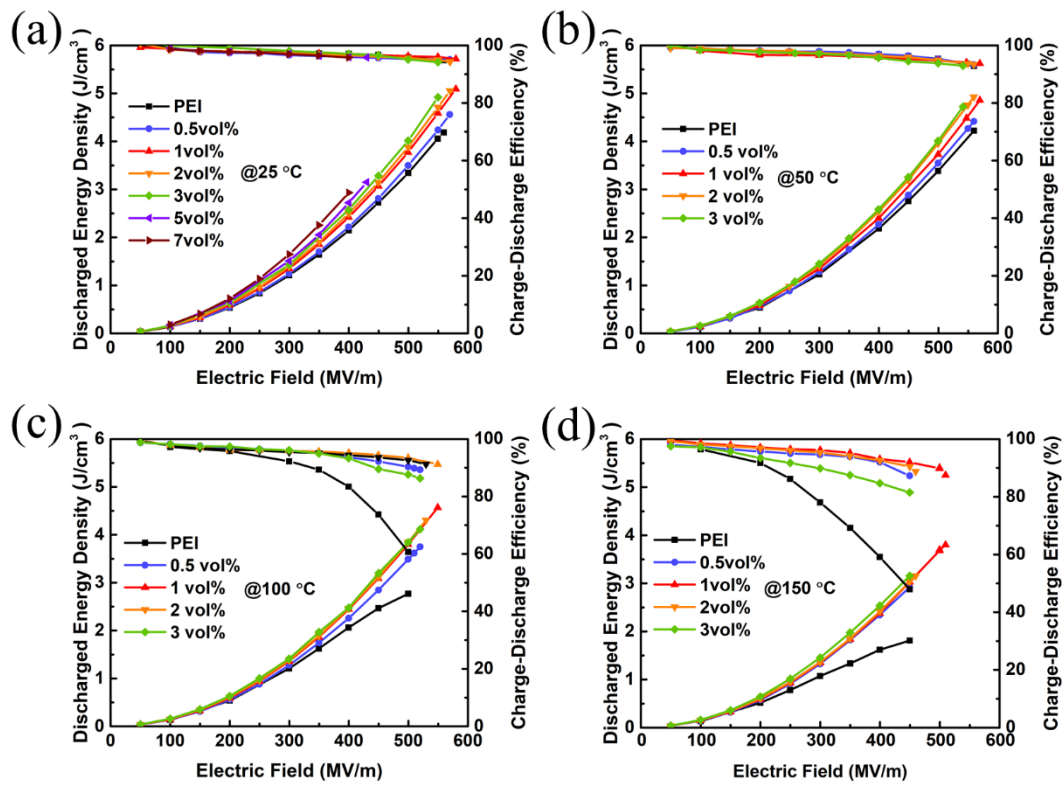


**Fig. S12.** Discharged energy density and charge-discharge efficiency of PEI/AO-nps nanocomposite films with varied filler contents measured at (a) 25 °C, (b) 50 °C, (c) 100 °C, and (d) 150 °C.

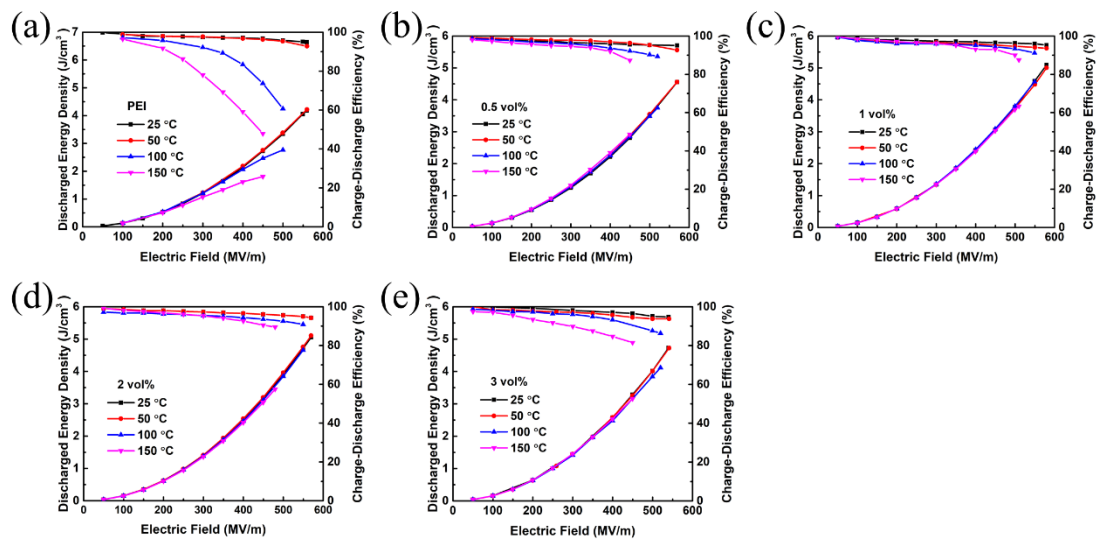


**Fig. S13.** Discharged energy density and charge-discharge efficiency of PEI/AO-nps nanocomposite films measured at different temperature, (a) PEI, (b) 0.5 vol%, (c) 1 vol%, (d) 2 vol%, and (e) 3 vol%.